

An analog cell to detect single event transients in voltage references[☆]

F. J. Franco^{a,*}, C. Palomar^a, J. G. Izquierdo^b, J. A. Agapito^a

^aDepartamento de Física Aplicada III, Facultad de Físicas, Universidad Complutense de Madrid (UCM), 28040 Madrid (Spain)

^bCentro de Láseres Ultrarrápidos, Facultad de Químicas, Universidad Complutense de Madrid (UCM), 28040 Madrid (Spain)

Abstract

A reliable voltage reference is mandatory in mixed-signal systems. However, this family of components can undergo very long single event transients when operating in radiation environments such as space, nuclear facilities, etc., due to the impact of heavy ions. The purpose of the present paper is to demonstrate how a simple cell can be used to detect these transients. The cell was implemented with typical COTS components and its behavior was verified by SPICE simulations and in a laser facility. Different applications of the cell are explored as well.

Keywords: Laser tests, long duration pulses, operational amplifiers, single event transients, voltage references

1. Introduction

Some electronic systems are designed to work in harsh environments, such as avionics, space, nuclear facilities or linear accelerators [1, 2]. In these environments, energetic heavy ions hit the electronic devices generating a high density of free carriers. If this happens in internal capacitances, such as gate oxides or reverse-biased PN junctions, the cloud is swept away by the electric field and an instantaneous current transient occurs, which is transmitted into the system.

With the exception of some mixed-signal components [3, 4], the only expected soft errors in analog devices are single event transients (SETs) due to the absence of memory elements. In particular, some works have reported that voltage references can show a very dangerous kind of SET called “long duration pulse” (LDP) [5, 6]. In special circumstances, the transients last for several hundreds of μs or even 1 ms. This characteristic is critical in analog-to-digital (A/D) or digital-to-analog (D/A) conversions [7]. In general, the output of a D/A or A/D converter is proportional to either V_{REF} or V_{REF}^{-1} . If a peak ΔV_{REF} appears, it is easy to demonstrate that the analog or digital output shows a percentage error of $\pm \frac{\Delta V_{REF}}{V_{REF}}$. Voltage references are usually built using a core cell (e.g., band-gap cells or Zener diodes) followed by an operational amplifier (op amp) (Fig. 1). The core cell provides a reference value (V_{CORE}) independent of the power supply or the temperature whereas the op amp stabilizes the system by negative feedback, scales the reference voltage, and improves the output characteristics. Usually, voltage references must provide current to the load. Thus, a simple class-A output stage is an efficient and widely-used solution (Q_O and I_Q in Fig. 1) [5].

[☆]This work was supported in part by the MCINN projects AYA2009-13300-C03-03 and Consolider SAUUL CSD2007-00013, by MCINN Grant CTQ2008-02578/BQU, and by UCM-BSCH.

*Corresponding author

Email address: fjfranco@fis.ucm.es (F. J. Franco)

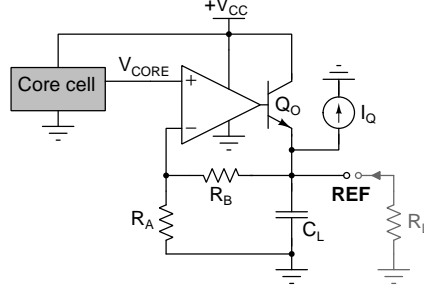


Figure 1: Standard voltage reference. A core cell, biased by the power supply, $+V_{CC}$, provides a stable voltage value (V_{CORE}) that works as the input of a non-inverting amplifier. Thus, $V_{REF} = \left(1 + \frac{R_B}{R_A}\right) \cdot V_{CORE}$. Typically, the output is just a class-A stage consisting of an NPN (or NMOS) transistor, Q_O , and a current source, I_Q , to bias it in the forward-active zone. The capacitor is included to filter noise. R_L represents a hypothetical load.

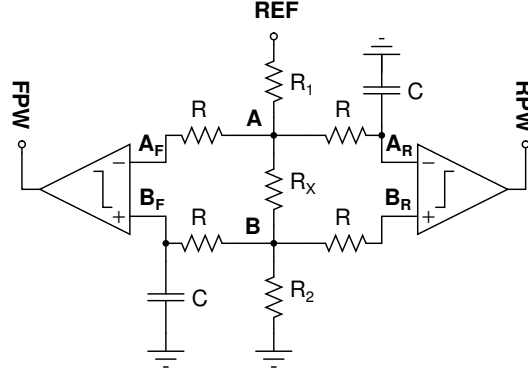


Figure 2: Proposed surveying cell. The output signals are the Rising Pulse Warning, RPW , and the Falling Pulse Warning, FPW . Some resistors are included to minimize the effects of the input bias currents. In comparators with open collector/drain output, additional pull-up resistors (R_{PU}) and a logic power supply ($+V_L$) are necessary.

LDPs in voltage references are a dangerous hazard since they lead to hundreds or thousands of erroneous conversions [5, 8]. In this paper, we are going to demonstrate how a very simple analog cell able to detect SETs beyond a tunable threshold value can help to solve this undesirable issue.

2. The cell and its properties

The proposed cell is shown in Fig. 2. In this cell, only passive components and two comparators are required. The input of the cell is REF and two warning digital signals (Rising Pulse Warning, RPW , and Falling Pulse Warning, FPW) are the outputs. Let us calculate the bias point, Q , accepting that the comparators have a high input impedance. It follows then that:

$$V_{A,Q} = \frac{R_2 + R_X}{R_T} \cdot V_{REF,Q} \quad (1)$$

$$V_{B,Q} = \frac{R_2}{R_T} \cdot V_{REF,Q} \quad (2)$$

R_T being $R_1 + R_2 + R_X$. At the bias point, $V_A = V_{AF} = V_{AR}$ and $V_B = V_{BF} = V_{BR}$ so $\Delta V_{BA} = -\frac{R_X}{R_T} \cdot V_{REF,Q} < 0$. Therefore, the outputs of both comparators are in the LOW state. Now, let us suppose that a transient occurs at REF . This transient can be modeled as a perturbation, $\pm v_{PK}$, around the bias point. Thus, during the transient,

37 $V_{REF}^* = V_{REF,Q} \pm v_{PK}$. The following step is to set the time constant, $\tau = R \cdot C$, much longer (e.g., one order of
 38 magnitude) than the worst-case transient duration. Given that the transient duration is $\sim 10\text{--}1000 \mu\text{s}$ [5, 6, 9], τ
 39 must be selected on the order of 0.1-10 ms. In this situation, the perturbation quickly reaches nodes A and B as
 40 well as nodes A_F and B_R , which are open circuits in practice. However, nodes A_R and B_F are not immediately
 41 affected due to the presence of the capacitors. Therefore, ΔV_{BA} becomes positive in one of the two comparators
 42 and its output switches to HIGH indicating the occurrence of an SET. Namely, rising transients, with $v_{PK} > 0$
 43 trigger RPW , whereas FPW is activated by falling transients.

44 Now, the cell will be analyzed in a quantitative way. Instead of resolving the circuit in the frequency domain,
 45 we are going to use the standard technique in the field of small-signal circuits research, which consists in modeling
 46 the capacitors as short-circuits in AC mode. Later, DC and AC contributions will be added using the superposition
 47 principle.

48 Hence, it can be demonstrated that one of the comparators is triggered if v_{PK} falls outside the interval
 49 $[-V_{THF}, V_{THR}]$ with:

$$V_{THR} \approx \frac{R_X}{R_2} \cdot V_{REF,Q} \quad (3)$$

$$V_{THF} \approx \frac{R_X}{R_2 + R_X} \cdot V_{REF,Q} \quad (4)$$

51 if $R \gg R_1, R_2$. Also, if $R = R_1 = R_2$:

$$V_{THR} \approx \frac{2R_X}{R} \left(1 + \frac{1}{2} \frac{R_X}{R}\right) \cdot V_{REF,Q} \quad (5)$$

$$V_{THF} \approx \frac{2R_X}{R} \left(1 - \frac{3}{2} \frac{R_X}{R}\right) \cdot V_{REF,Q} \quad (6)$$

53 Anyhow, if $R_X \ll R_2$, $V_{THR} \approx V_{THF}$. An interesting feature is that, as the thresholds are defined as percentage
 54 values, the cell functions whatever the reference voltage. Finally, the analysis remains valid once the network has
 55 reached the bias point. Therefore, the cell does not work immediately after powering-up the system, the delay being
 56 on the order of τ .

57 It is interesting to check how non-idealities compromise the performance of the cell. First of all, let us investigate
 58 the effects of the resistor tolerance. For the sake of brevity, only the situation in which $R \gg R_1, R_2$ will be described.
 59 According to the error propagation theory, the uncertainty of V_{THR} , ΔV_{THR} , is related to the resistor tolerance as:

$$\frac{\Delta V_{THR}}{V_{THR}} = \frac{\Delta R_X}{R_X} + \frac{\Delta R_2}{R_2} \quad (7)$$

60 as it is easily deduced from Eq. 3. Therefore, precision resistors are strongly recommended.

61 Another interesting parameter to take into account is the input offset voltage of the comparators. For example,
 62 if $R \gg R_1, R_2$, the rising transients are detected if:

$$v_{PK} > V_{THR} + \frac{R_T}{R_2} \cdot V_{OS,R} \quad (8)$$

63 and the falling ones if:

$$|v_{PK}| > V_{THF} + \frac{R_T}{R_2 + R_X} \cdot V_{OS,F} \quad (9)$$

64 $V_{OS,R}$ and $V_{OS,F}$ being the input offset voltages of the comparators that detect **R**ising and **F**alling transients.
 65 Another parameter that can affect the performance of the cell is the input bias current of the comparators. In Fig.
 66 2, we can see that every input of the comparators is connected to the nodes AF, AR, BF and BR. This will be the
 67 guideline to denominate the corresponding input bias currents. Defining them positive if flowing into the device,
 68 calculations show that they contribute to the effective input offset voltage as:

$$\Delta V_{OS,R}^* = \frac{R_X}{R_T} [R_2 \cdot (I_{BF} + I_{BR}) - R_1 \cdot (I_{AF} + I_{AR})] - R \cdot (I_{BR} - I_{AR}) \quad (10)$$

$$\Delta V_{OS,F}^* = \frac{R_X}{R_T} [R_2 \cdot (I_{BF} + I_{BR}) - R_1 \cdot (I_{AF} + I_{AR})] - R \cdot (I_{BF} - I_{AF}) \quad (11)$$

70 The influence of the input bias currents is minimized if currents are extremely low or, if $R_1 = R_2$, identical to cancel
 71 each other out.

72 3. Simulations in SPICE

73 In order to verify the functioning of the analog cell we carried out simulations using realistic SPICE models
 74 of commercial-off-the-shelf (COTS) discrete components found in the literature on electronic systems for space.
 75 The voltage reference was created using an LM124A SPICE micromodel in non-inverting configuration, which is
 76 an improved version of the one that was successfully used by the authors to investigate SETs in networks with op
 77 amps [6, 10, 11].

78 Concerning the output stage, the NPN transistor was modeled as a typical 2N2222A. Furthermore, the current
 79 source, I_Q , was removed since the feedback resistor network, R_A and R_B , managed to correctly bias the transistor
 80 in forward-active zone. Other parameters of the simulated voltage reference were $V_{CORE} = 1.25$ V, $R_A = 33$ k Ω ,
 81 $R_B = 100$ k Ω , which yield $V_{REF} = 5.0$ V.

82 The cell was implemented using an LM311-like voltage comparator, depicted in [12, 13]. In this case, the SPICE
 83 micromodel was developed from the detailed schematic in the manufacturer's datasheet with identical transistor
 84 models to those of the LM124A micromodel. Current mirrors biasing the different stages were fitted from the
 85 original works by R. Widlar [14, 15]. As the comparator has an open-collector output, an additional pull-up resistor
 86 of 10 k Ω was necessary in the simulations.

87 Different combinations of R_L (0.1, 0.47, 1, and 4.7 k Ω) and C_L (0.1, 0.22, 0.47, and 1.0 μ F) were used in the
 88 simulations to verify the correct operation of the cell. However, in this paper only the results associated with
 89 $C_L = 100$ nF and $R_L = 4.7$ k Ω will be shown. The reason of selecting this resistance value is that it is on the
 90 order of the equivalent load of, e. g., typical R/2R networks in DACs [16, 17]. Finally, the simulation engine was
 91 NGSPICE rework 26, a GNU fork of Berkeley SPICE 3f5¹.

92 SETs were simulated by means of piece-wise current sources between the reverse biased CB junctions of bipolar
 93 transistors in forward active or cut-off zone. In particular, the rising transients were emulated by draining 0.4 pC
 94 from a specific transistor of the gain stage, $QR1$, and the falling ones by draining 3 pC from a neighbor transistor,
 95 $Q09$, also in the gain stage [6, 10, 11]. Preliminary simulations showed that the duration of the longest transient

¹<http://ngspice.sourceforge.net>

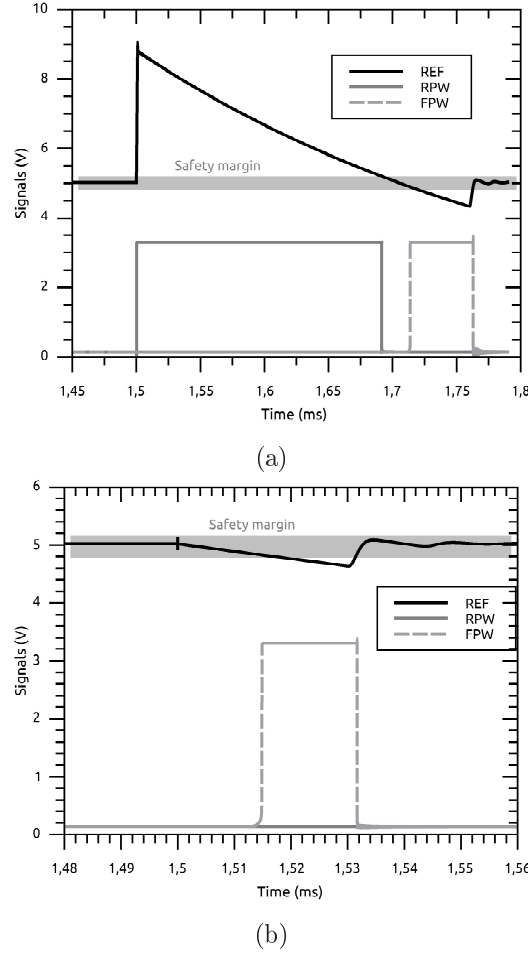


Figure 3: Response of the surveying cell in case of simulated SETs.

was below $250 \mu s$. This value was necessary to determine the network parameters in Fig. 2, which were eventually chosen as $V_L = 3.3 V$, $R_1 = R_2 = 10 k\Omega$, $R_X = 200 \Omega$, $R = 10 k\Omega$, and $C = 220 nF$. Therefore the threshold value was set around 200 mV and τ near 2.2 ms. Fig. 3a-b shows the response of the cell when rising (in reality, bipolar) or falling SETs occur, demonstrating that the cell apparently operates as expected. Every time the voltage reference output leaves the safety margin, $5 V \pm 200 mV$ (gray zone in both graphs), one of the logic signals switches to HIGH.

Finally, we would like to clarify the reasons for our choice of components. In actual designs, a dedicated voltage reference (discrete or that included in usual D/A or A/D converters) must be used instead of the system built with the LM124A and accessories. In this work, the voltage reference is built as described only for illustrating purposes. In fact, realistic transients are easily induced in this system and can be used to test the analog cell in typical conditions. Moreover, the LM311 was selected since it is still used in some designs and its behavior under radiation is well understood. Other newer, faster, and more reliable voltage comparators can be used in custom implementations.

109 4. Experimental results

110 Even though the theoretical behavior of the cells is quite simple and has been corroborated by simulations, the
 111 conclusive test is to confront the cell with an actual SET. An interesting and cheap option to induce SETs are laser
 112 facilities, which have become an excellent option to study heavy ions effects. These tests are specially accurate in
 113 old bipolar technologies, with transistor sizes of some tens of μm [18]. The laser wavelength at the UCM-CLUR
 114 [6, 10] was 800 nm, and the spot size of the focused laser was around 1 μm , much smaller than the typical transistors
 115 that make up the LM124A. The laser setup is thoroughly explained in other works by the authors [6, 10, 11, 13].

116 As in the simulations, the voltage reference was built using an LM124A as core op amp, biased by a unipolar 12-V
 117 power supply. External parameters were chosen identical to those of the simulations but, due to technical reasons,
 118 the voltage reference was build with two Si diodes in series configuration in such a way that $V_{REF} \approx 5.4\text{ V}$. Finally,
 119 V_L , or logic power supply, was set to +5 V. The LM124A, in ceramic package, was decapsulated mechanically to
 120 make the internal devices accessible. $QR1$ and $Q09$ were located on the surface of the decapsulated LM124A as
 121 shown in [6, 10] and illuminated by the laser light (Energy $\sim 50\text{ pJ}$). According to [5, 8], the laser is equivalent to a
 122 heavy ion with $\text{LET} \sim 50\text{ MeV}\cdot\text{cm}^2/\text{mg}$. Results are shown in Fig. 4a-b. Both graphs demonstrate that the analog
 123 cell does detect SETs raising one of the outputs from LOW to HIGH. For the sake of clarity, only one of the digital
 124 signals is shown in each graph.

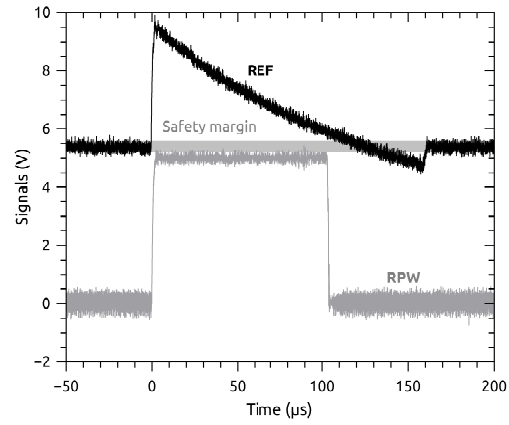
125 The cell was tested with different combinations of R_L (0.1, 0.47, 1, and 4.7 k Ω) and C_L (0.1, 0.22, 0.47, and
 126 1.0 μF) and the detection was always correctly done. Only when the transient was very long ($\sim 100\text{ }\mu\text{s}$), the signal
 127 apparently switched to LOW state before REF returned to the safety margin. This is attributed to the slow but
 128 unavoidable accumulation of charge in the capacitors, which shifts the threshold levels upwards.

129 An interesting point is the delay between the transients and the logic signals. Defining $t_{50\%}$ as the time needed
 130 by the comparator to reach 50% of the final logic value (2.5 V), the LM311 delay ranged from 0.6 to 0.8 μs depending
 131 on the value of the pull-up resistor. At any rate, this delay is much shorter than the transient duration (some tens or
 132 hundreds of μs). On the other hand, switching from HIGH to LOW is almost instantaneous whatever the pull-up
 133 output resistor is. This delay should be shorter if this comparator is replaced by more advanced components.

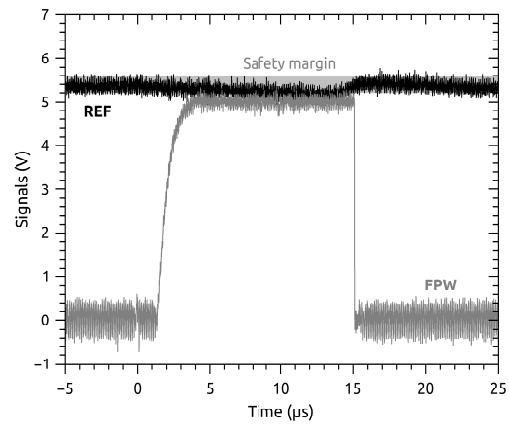
134 5. Discussion

135 5.1. Load effects

136 Several factors must be studied before using this cell in actual systems. First of all, it is necessary to determine
 137 how the cell affects the surveyed voltage reference. The load regulation is a typical parameter of voltage references
 138 that evaluates the voltage drop associated with the output current. Typical commercial voltage references such as
 139 the 5-V REF02 have a load regulation value below 0.01 %/mA. Accepting this value, the actual analog cell tested
 140 in the laser facility ($R_1 = R_2 = 10\text{ k}\Omega$, $R_X = 100\text{ }\Omega$, $R_T = 20.1\text{ k}\Omega$) induces a negligible drop of $\sim 100\text{ }\mu\text{V}$.
 141 However, voltage references liable to undergo SETs could be used in environments where total ionizing dose (TID)
 142 or displacement damage (DD) are expected (e.g., space, nuclear facilities, etc.). The load regulation is a parameter
 143 that increases with the permanent radiation damage. Even more, in very irradiated devices, the output stage of
 144 the voltage reference is so damaged that it cannot provide enough current to bias load resistors even on the order
 145 of 10 k Ω [17, 19].



(a)



(b)

Figure 4: Response of the surveying cell in actual SETs. For the sake of clarity, only the main warning signal is shown.

Finally, in spite of the fact that the cell is a two-pole/two-zero network, spontaneous oscillations were not observed during the tests whatever the values of R_L and C_L were.

5.2. Reliability of the cell

Additionally, it is reasonable to assume that the analog cell is exposed to the same kind of radiation as the surveyed voltage reference. First of all, SETs can occur also in the comparators. However, there are some reasons to believe that this is a minor threat. In the LM111 family, LOW-to-HIGH transients are typically very short ($\tau \lesssim 1 \mu s$) and can even disappear if the pull-up resistor is large enough [12, 13, 20]. On the contrary, transients in voltage references can last for tens or hundreds of μs [5]. Besides, the threshold linear energy transfer (LET) value of the comparators dramatically decreases if the input voltage difference moves away some tens of mV from the switch threshold [20]. Finally, as it is shown in the following section, some applications are hardly affected by these transients.

Also, voltage comparators can experience an offset voltage drift as well as an increase of the input bias currents due to accumulated damage (TID, DD) [21]. The influence of the input offset voltage increase is enhanced in case of choosing a very large value of R_1 as deduced from Eq. 8 and 9. Besides, Eq. 10-11 shows that, if the currents are identical in the four inputs and $R_1 = R_2$, their influence vanishes. To conclude, as the input voltage difference is some tens of volts at the most, pernicious effects related to the asymmetric polarization of the inputs seem to be unlikely [21].

5.3. Mitigation of SETs

In voltage references, rising transients are very long due to the trapped charge inside the load capacitor (C_L in Fig. 1) [5, 6, 11]. A simple way to mitigate the transients is using the RPW signal to activate a low impedance path to drain the capacitor (e.g. the NMOS in Fig. 5a). This structure was tested in the laser facility using the IRFD014, a commercial discrete NMOS transistor, and $R_P = 100 \Omega$. Fig. 5b shows the signals obtained with identical loads to those of Fig. 4a. The first conclusion is that the peak voltage hardly changes from Fig. 4a to Fig. 5b. Unfortunately, this strategy makes the transient shorter but not smaller. Second, the RPW signal rises more slowly due to the influence of the parasitic capacitor at the NMOS transistor gate. Finally, the transient duration is reduced from $150 \mu s$ to hardly $30 \mu s$. Even more, the most significant initial positive peak is reduced from $110 \mu s$ to $12 \mu s$.

The transient detection is more effective if FPW and RPW signals are NORed to create a single warning signal, $WARN$. For instance, microprocessors or FPGAs that process the digital signal coming from an ADC can use the $WARN$ signal to dismiss data obtained during the transient. Moreover, combined with a backup voltage reference, it can be used to set a constant value of reference voltage independently of the occurrence of SETs. The idea is shown in Fig. 6. If the $REF1$ signal is correct, $FPW = RPW = LOW \rightarrow WARN = HIGH$. In case a transient occurs at $REF1$, the NOR gate output switches to LOW activating a single pole, double throw (SPDT) switch that selects a backup reference voltage, $REF2$. Formally, the system compares $REF1$ with its copies in the capacitors and, in case of disagreement, the system selects the third option, $REF2$. Defining $REFC$ as the voltage in the capacitors, it is easy to deduce that REF is the output of the algorithm

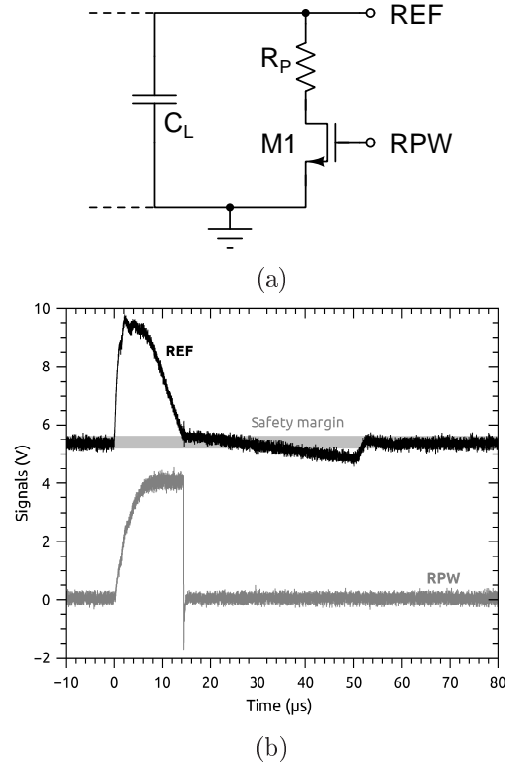


Figure 5: Mitigation of transients using the analog cell. An NMOS, controlled by the RPW signal, is in OFF state and switches to linear zone if $RPW = HIGH$ (a). The second graph shows the mitigated transient (b).

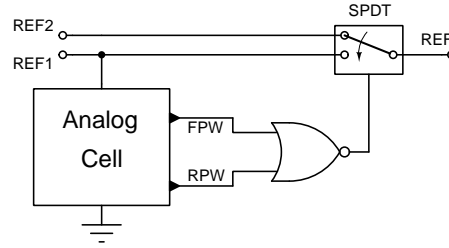


Figure 6: A circuit to keep the reference voltage constant.

182
$$\text{if } (REF1 = REFC) \text{ then } REF = REF1$$

183
$$\text{else } REF = REF2$$

184 If $REF1$, $REFC$, and $REF2$ were logic signals instead of analog ones, the algorithm would be formally equivalent
 185 to a majority voter for Triple Modular Redundancy (TMR).

186 Transients are rare events so it is very improbable that both references fail simultaneously. Typically, COTS
 187 components appropriate for this circuit are built in high-voltage CMOS technologies. However, if damage by
 188 accumulated radiation is expected, the NOR gate can be chosen from the SiGe family [22, 23] while the analog
 189 switch can be the SW06, with only bipolar and JFET transistors and therefore very tolerant to TID damage.
 190 Finally, it must be taken into account that SETs in the comparators or the NOR gate do not affect the effective
 191 output (REF in Fig. 6).

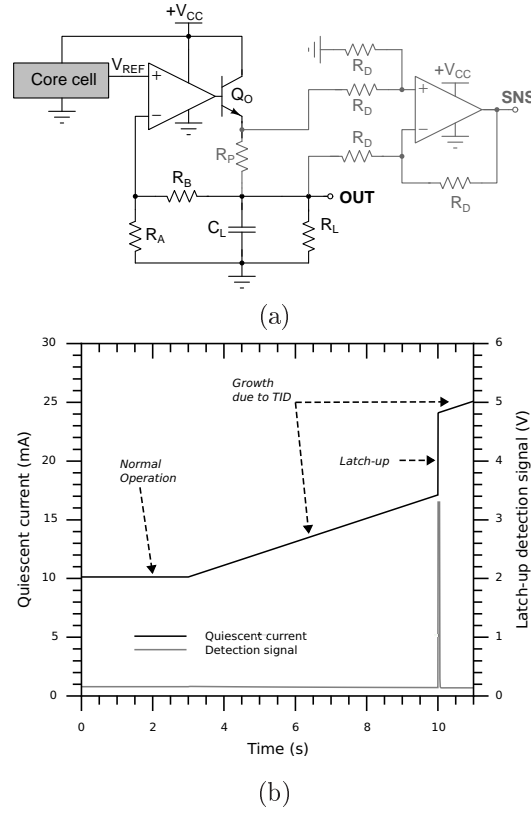


Figure 7: Typical circuit (in gray) to measure the quiescent current needed by a load (a). SPICE simulation of the behavior of the analog cell which surveys the SNS signal (b). From $t = 3$ s on, the quiescent current slowly increases due to a TID damage, but the cell is not triggered. At $t = 10$ s, a latch-up occurs and is detected by the cell ($R_1 = R_2 = R = 10 \text{ k}\Omega$, $R_X = 100 \Omega$, $C_L = 1 \mu F$, $R_P = 100 \Omega$, and $R_D = 20 \Omega$).

5.4. Other potential applications

The cell can also be useful during the preparation of heavy-ion or laser tests. When a researcher wants to characterize an analog device with a constant output value in a radiation facility, the typical procedure consists in setting the oscilloscope trigger to a threshold level and register every transient going beyond this level. Unfortunately, some low-end oscilloscopes have no bipolar trigger. In other words, they can be set to detect rising or falling transients, but not both simultaneously. The analog cell solves this problem since the $WARN$ signal can trigger the oscilloscope whichever the kind of transient is.

Another application is the detection of latch-up in accelerated radiation tests. One of the advantages of the cell is its independence of the DC level of the surveyed voltage signal. Also, shifts in this voltage are not detected if they are slow. Fig. 7a shows a differential amplifier measuring the voltage drop across a sense resistor, R_P . The output voltage, V_{SNS} , which is proportional to the output current, is surveyed by the analog cell. SPICE simulation results are shown in Fig. 7b. One can see that the analog cell is only triggered by the latch-up and not by the slow drift. Obviously, this detection technique is only appropriate for static tests as the cell will show false detections if there are sudden requirements of current (e. g., while writing/reading a memory).

206 6. Conclusion

207 A simple analog cell is proposed to detect single event transients in voltage references. This cell was implemented
 208 with discrete passive components and two typical voltage comparators and its correct functioning demonstrated by
 209 means of SPICE simulations and in a laser facility. Also, it can be used to mitigate the transients making their
 210 duration much shorter or to select a backup voltage reference in case the main one fails. Finally, it can simplify
 211 the setup of static tests of components in heavy-ion or laser facilities since it allows the use of low-end oscilloscopes
 212 and the simple detection of latch-up.

213 References

- 214 [1] S. Duzellier, Radiation effects on electronic devices in space, *Aerospace Science and Technology* 9 (1) (2005)
 215 93–99. doi:10.1016/j.ast.2004.08.006.
- 216 [2] M. Brugger, Radiation Damage to Electronics at the LHC, in: 3rd Int. Particle Accelerator Conf., no. CERN-
 217 ATS-2012-255, 2012, pp. 3734–3736.
 218 URL <http://cds.cern.ch/record/1481526?ln=es>
- 219 [3] A. Zanchi, S. Buchner, S. Hisano, A. Wilson, C. Hafer, D. B. Kerwin, A Comprehensive Methodology to
 220 Rate SETs of Complex Analog and Mixed-Signal Circuits Demonstrated on 16-bit A-to-D Converters, *IEEE*
 221 *Transactions on Nuclear Science* 59 (6) (2012) 2739–2747. doi:10.1109/TNS.2012.2222926.
- 222 [4] H. Venkatram, J. Guerber, M. Gande, U.-K. Moon, Detection and Correction Methods for Single Event Effects
 223 in Analog to Digital Converters, *IEEE Transactions on Circuits and Systems I: Regular Papers* 60 (12) (2013)
 224 3163–3172. doi:10.1109/TCSI.2013.2265963.
- 225 [5] A. Zanchi, S. Buchner, C. Hafer, S. Hisano, D. Kerwin, Investigation and Mitigation of Analog SET on
 226 a Bandgap Reference in Triple-Well CMOS Using Pulsed Laser Techniques, *IEEE Transactions on Nuclear*
 227 *Science* 58 (6) (2011) 2570–2577. doi:10.1109/TNS.2011.2172460.
- 228 [6] C. Palomar, F. J. Franco, I. Lopez-Calle, J. G. Izquierdo, J. A. Agapito, Peak Detector Effect in Low-Dropout
 229 Regulators, *IEEE Transactions on Nuclear Science* 60 (4) (2013) 2666–2674. doi:10.1109/TNS.2012.2232305.
- 230 [7] T. C. Carusone, D. Johns, K. Martin, *Analog Integrated Circuits*, 2nd Edition, John Wileys and Sons, Inc.,
 231 2013.
- 232 [8] A. Zanchi, S. Buchner, Y. Lotfi, S. Hisano, C. Hafer, D. Kerwin, Correlation of Pulsed-Laser Energy and Heavy-
 233 Ion LET by Matching Analog SET Ensemble Signatures and Digital SET Thresholds, *IEEE Transactions on*
 234 *Nuclear Science* 60 (6) (2013) 4412–4420. doi:10.1109/TNS.2013.2279653.
- 235 [9] P. Adell, L. Scheick, Radiation Effects in Power Systems: A Review, *IEEE Transactions on Nuclear Science*
 236 60 (3) (2013) 1929–1952. doi:10.1109/TNS.2013.2262235.

- [10] F. J. Franco, I. Lopez-Calle, J. G. Izquierdo, J. A. Agapito, Modification of the LM124 Single Event Transients by Load Resistors, *IEEE Transactions on Nuclear Science* 57 (1) (2010) 358–365. doi:10.1109/TNS.2009.2037894.
- [11] C. Palomar, F. J. Franco, J. G. Izquierdo, I. Lopez, J. A. Agapito, Characteristics of the long duration pulses in a shunt linear voltage regulator, *Nuclear Instruments and Methods in Physics Research Section A: Accelerators, Spectrometers, Detectors and Associated Equipment* 737 (0) (2014) 273–280. doi:10.1016/j.nima.2013.11.083.
- [12] I. Lopez-Calle, et al., TPA laser source for SEE test at UCM, in: 12th European Conf. on Radiation and Its Effects on Components and Systems (RADECS2011), 2011, pp. 454–457. doi:10.1109/RADECS.2011.6131421.
- [13] I. Lopez-Calle, F. J. Franco, J. A. Agapito, J. G. Izquierdo, Load resistor as a worst-case parameter to investigate single-event transients in analog electronic devices, in: 2011 IEEE Spanish Conf. on Electron Devices, 2011, pp. 1–4. doi:10.1109/SCED.2011.5744202.
- [14] R. J. Widlar, An IC Voltage Comparator for High Impedance Circuitry. National-Semiconductor App. Not. LB-12 (January 1970).
URL <http://www.national.com/an/LB/LB-12.pdf>
- [15] R. J. Widlar, Precision IC Comparator Runs from +5V Logic Supply. National-Semiconductor App. Not. AN-41 (October 1970).
URL <http://www.national.com/an/AN/AN-41.pdf>
- [16] F. Franco, J. Lozano, J. Agapito, Radiation effects on CMOS R/2R ladder digital-to-analog converters, in: Proceedings of the 7th European Conference on Radiation and Its Effects on Components and Systems (RADECS 2003), 2003, pp. 571–578.
- [17] F. J. Franco, Y. Zong, J. A. Agapito, J. G. Marques, A. C. Fernandes, J. Casas-Cubillos, M. A. Rodriguez-Ruiz, Radiation tolerant D/A converters for the LHC cryogenic system, *Nuclear Instruments and Methods in Physics Research Section A: Accelerators, Spectrometers, Detectors and Associated Equipment* 553 (3) (2005) 604–612.
- [18] S. Buchner, F. Miller, V. Pouget, D. McMorro, Pulsed-Laser Testing for Single-Event Effects Investigations, *IEEE Transactions on Nuclear Science* 60 (3) (2013) 1852–1875. doi:10.1109/TNS.2013.2255312.
- [19] F. J. Franco, Y. Zong, J. A. Agapito, A. H. Cachero, Radiation effects on XFET voltage references, in: IEEE Radiation Effects Data Workshop, 2005, pp. 138–143. doi:10.1109/REDW.2005.1532680.
- [20] S. LaLumondiere, R. Koga, P. Yu, M. Maher, S. Moss, Laser-induced and heavy ion-induced single-event transient (SET) sensitivity measurements on 139-type comparators, *IEEE Transactions on Nuclear Science* 49 (6) (2002) 3121–3128. doi:10.1109/TNS.2002.805414.
- [21] M. F. Bernard, L. Dusseau, J. Boch, J.-R. Vaille, F. Saigne, R. Schrimpf, E. Lorfèvre, J.-P. David, Analysis of Bias Effects on the Total-Dose Response of a Bipolar Voltage Comparator, *IEEE Transactions on Nuclear Science* 53 (6) (2006) 3232–3236. doi:10.1109/TNS.2006.885002.

- 271 [22] J. Cressler, Silicon-Germanium as an Enabling Technology for Extreme Environment Electronics, IEEE Trans-
272 actions on Device and Materials Reliability 10 (4) (2010) 437–448. doi:10.1109/TDMR.2010.2050691.
- 273 [23] J. Cressler, Radiation Effects in SiGe Technology, IEEE Transactions on Nuclear Science 60 (3) (2013) 1992–
274 2014. doi:10.1109/TNS.2013.2248167.